Electronic Supplementary Information: Soft-solid deformation mechanics at the tip of an embedded needle

Shelby B. Hutchens and Alfred J. Crosby

1 FE Convergence Study

Figure S1 plots the results of FE simulation results for increasing mesh-resolution (decreasing element size) providing evidence that the mesh size chosen is sufficiently refined.

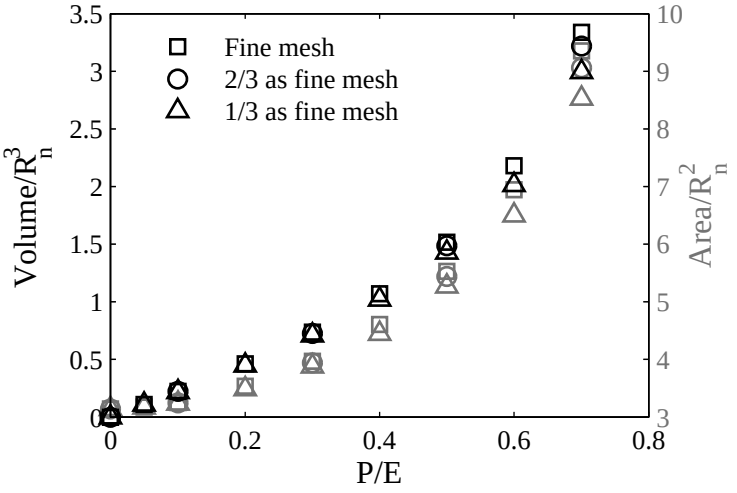

Figure S1: Demonstration of the convergence of volume, V, (black) and area, A, (grey) of the void formed at the tip of and embedded-needle FE calculation as a function of mesh refinement at a series of applied, normalized pressure values P/E.

2 Spherical Indenter FE Simulations

A pressurized void at the tip of a needle is expected assume the shape of a spherical cap in the limit of large γ/EA. Utilizing identical boundary conditions and element sizes to those outlined in the main text (Section 2), FE simulations of a spherical cap-shaped analytical surface displaced into the surface of the material at the tip of the embedded needle are performed. Contact between the two surfaces is frictionless. In order to compare these displacement controlled void calculations with the pressure-stretch response obtained previously, we take the applied pressure to be the z-direction reaction force on the spherical cap indenter divided by the area at the tip of the needle. Figure S2 shows the void surface profiles obtained for spherical cap indenters up to a maximum displacement, d/R_n, of 0.9. Spherical caps with larger than hemisphere ($d/R_n = 1$) volumes were unable to be simulated due to geometric restrictions.

The spherical cap-shaped indenter provides a limiting case from which to evaluate the uncertainty associated with utilizing an elastic-only response to model void deformation at the tip of a needle. Large stretch ratios cannot be achieved with this approximation, nevertheless, P_{max} occurs at relatively small stretch ratios,

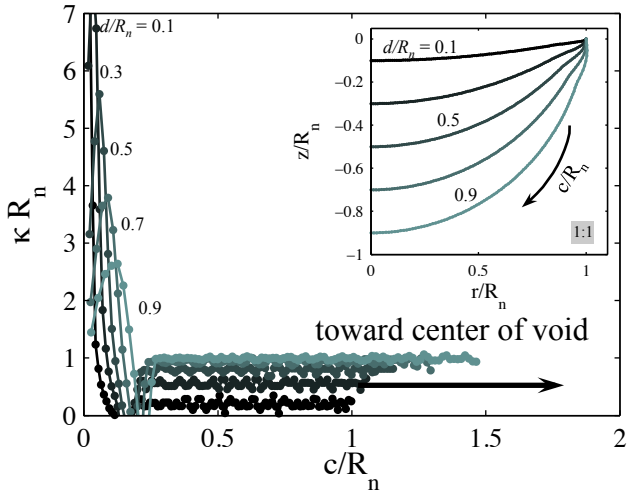

Figure S2: Curvature as a function of contour length, c, along the void surface for normalized center displacement, $d/R_n = 0.1$, 0.3, 0.5, 0.7, and 0.9. Inset: Evolution of the void geometry for $d/R_n = 0.01$, 0.3, 0.5, 0.7, and 0.9.

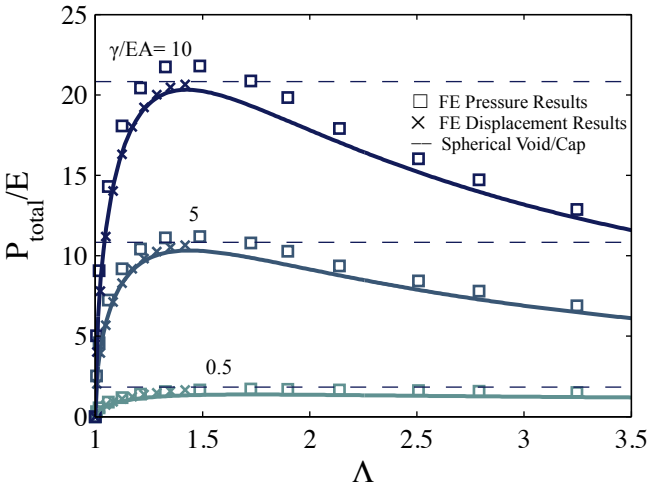

Figure S3: Total pressure ($P/E + P_{\text{Laplace}}/E$) versus stretch curves for FE simulations obtained via a pressurized void (squares), a spherical cap (x's), and the analytical spherical void plus spherical cap approximation (lines) for three different values of γ/EA, 0.5, 5, and 10, corresponding to an increasing importance of surface tension. Dashed lines correspond to P_{max} as predicted by the 'cavitation equation' (Eq. (3)).

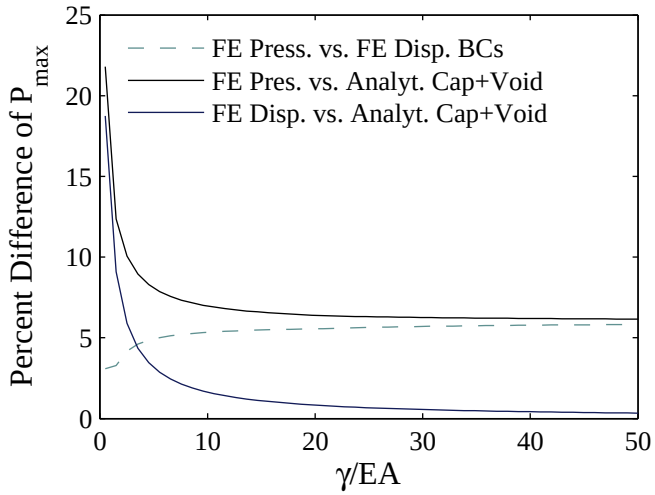

Figure S4: Percent differences between P_{max} values calculated using all three approximations. Differences between FE pressurized void (black) and FE spherical indenter (blue) are shown in solid lines. The difference between the maximum values predicted using the two different FE approximations is shown in a teal dashed line.

$\Lambda < 2$, for which pressure-stretch relationships can be obtained. Therefore, P_{max} values can be compared between the three calculation scenarios: FE pressurized void, FE spherical-cap void, and analytical spherical void/spherical cap, to evaluate the percent difference between these approximations and therefore the uncertainty associated with relying on the FE pressurized void. The total pressure versus stretch values for the analytical spherical void/spherical cap approximation, the pressurized FE simulation (Fig. 2), and the spherical cap displacement FE simulation are shown in Figure S3. The differences between these various calculations are minimal as illustrated in Figure S4, which quantifies the percent difference between the maximum pressure, P_{max}, found for each calculation method. Note that the values presented in Fig. S4 are percent differences among different calculation scenarios. They are not directly percent error for Eq. (3). Importantly, the greatest percent difference occurs for values of $\gamma/EA < 3$ for which the elastic-only FE response modeled would be expected to even more accurately describe void deformation in comparison to a spherical cap-like void. From this we can conclude that it is unnecessary to completely capture the details of the void shape in the intermediate range in which surface tension forces and elasticity contribute equally to void deformation since the error in using Eq. (3) is still well within experimental resolution.